HHS Public Access

Author manuscript

J Cardiovasc Electrophysiol. Author manuscript; available in PMC 2017 October 01.

Published in final edited form as:

J Cardiovasc Electrophysiol. 2016 October ; 27(10): 1220–1229. doi:10.1111/jce.13049.

Increased Susceptibility to Atrial Fibrillation Secondary to Atrial Fibrosis in Transgenic Goats Expressing Transforming Growth Factor-β1

Irina A. Polejaeva, Ph.D.[#†], **Ravi Ranjan, M.D., Ph.D.**[#‡,¶], **Christopher J. Davies, D.V.M., Ph.D.**[†], **Misha Regouski, B.S.**[†], **Justin Hall, M.S.**[†], **Aaron L. Olsen, D.V.M., Ph.D.**[†], **Qinggang Meng, Ph.D.**[†], **Heloisa M. Rutigliano, D.V.M., Ph.D.**[†], **Derek J. Dosdall, Ph.D.**[§], **Nathan A. Angel, Ph.D.**[‡], **Frank B. Sachse, Ph.D.**[‖,¶], **Thomas Seidel, M.D.**[‖], **Aaron J. Thomas, Ph.D.**[†], **Rusty Stott, D.V.M.**[†], **Kip E. Panter, Ph.D.**[##], **Pamela M. Lee, D.V.M.**[††], **Arnaud J. Van Wettere, D.V.M, Ph.D.**[†], **John R. Stevens, Ph.D.**[‡‡], **Zhongde Wang, Ph.D.**[†], **Rob S. MacLeod, Ph.D.**[‡,‖], **Nassir F. Marrouche, M.D.**[‡], and **Kenneth L. White, Ph.D.**[†]

[†]Department of Animal, Dairy and Veterinary Sciences, Utah State University, Logan, UT

[‡]CARMA Center, Division of Cardiology, University of Utah, Salt Lake City, UT

[§]Center for Engineering Innovation, University of Utah, Salt Lake City, UT

[‖]Nora Eccles Harrison Cardiovascular Research and Training Institute, University of Utah, Salt Lake City, UT

[¶]Department of Bioengineering, University of Utah, Salt Lake City, UT

[##]USDA ARS Poisonous Plant Research Laboratory, Logan, UT

[††]College of Veterinary Medicine, Washington State University, Pullman, WA

[‡‡]Department of Mathematics and Statistics, Utah State University, Logan, UT

[#] These authors contributed equally to this work.

Abstract

Introduction—Large animal models of progressive atrial fibrosis would provide an attractive platform to study relationship between structural and electrical remodeling in atrial fibrillation (AF). Here we established a new transgenic goat model of AF with cardiac specific overexpression of TGF-β1 and investigated the changes in the cardiac structure and function leading to AF.

Methods and Results—Transgenic goats with cardiac specific overexpression of constitutively active TGF-β1 were generated by somatic cell nuclear transfer. We examined myocardial tissue, ECGs, echocardiographic data, and AF susceptibility in transgenic and wild-type control goats. Transgenic goats exhibited significant increase in fibrosis and myocyte diameters in the atria compared to controls, but not in the ventricles. P-wave duration was significantly greater in

Address for correspondence: Irina A. Polejaeva, PhD, 4815 Old Main Hill, Logan, UT, USA 84322-4815. FAX: (435) 797-2118, Phone: (435) 797-3718 irina.polejaeva@usu.edu.

Drs. Polejaeva & Davies report patent filed by Utah State University related to the production of the goat animal model in this study. Dr. Sachse reports research support from Medtronic for pacemakers donation. Other authors: No disclosures.

transgenic animals starting at 12-month of age, but no significant chamber enlargement was detected, suggesting conduction slowing in the atria. Furthermore, this transgenic goat model exhibited a significant increase in AF vulnerability. Six of 8 transgenic goats (75%) were susceptible to AF induction and exhibited sustained AF (>2 minutes), whereas, none of 6 controls displayed sustained AF ($P<0.01$). Length of induced AF episodes was also significantly greater in the transgenic group compared to controls (687±212.02 vs. 2.50±0.88 seconds, $P<0.0001$), but no persistent or permanent AF was observed.

Conclusion—A novel transgenic goat model with a substrate for AF was generated. In this model, cardiac overexpression of TGF-β1 led to an increase in fibrosis and myocyte size in the atria, and to progressive P-wave prolongation. We suggest that these factors underlie increased AF susceptibility.

Keywords

Atrial Fibrillation; fibrosis; TGF-β1 transgenic goat model; genetics

Introduction

Atrial fibrillation (AF) is the most common sustained cardiac arrhythmia, with significant morbidity and mortality.[1] Ablation is routinely used to treat AF but long-term success especially for persistent AF is poor ranging from 40 to 60%, frequently after multiple ablations.[2, 3] Studies on patients, large animal models and transgenic mouse models have shown a strong association of atrial fibrosis with atrial fibrillation.[4, 5] In fact, these studies have shown that atrial fibrosis increases AF vulnerability.[6, 7] Nevertheless, the mechanisms of AF and its relationship with fibrosis are not well understood, in part because of suboptimal animal models. Transforming growth factor β1 (TGF-β1) is an essential mediator of atrial fibrosis in animal models[8, 9] and human patients.[10-12] Mice that overexpress active TGF-β1 have profound atrial fibrosis and increased susceptibility to AF induction via rapid atrial pacing (RAP).[8] Transgenic mouse models have provided vital information about the events that lead to AF[8, 13-15], but the small heart size makes them unsuitable for intracardiac mapping or testing new ablation therapies.

Large animal models of AF more closely resemble AF in humans and allow for sustained induction of AF[13] as compared to rodent models.[8] Rapid atrial pacing models (goat[16, 17] and dog[6] models) typically do not exhibit increased perimysial fibrosis, a hallmark of normal aging.[18] Atrial fibrosis observed in several large animal models of other experimentally induced pathologies (e.g., heart failure model[9] or hypertension[19]). As AF is often not accompanied by other diseases (e.g., prevalence of AF in heart failure studies ranges from 13 to 27%),[20] the development of an animal model with genetically induced progressive atrial fibrosis that would lead to increase AF susceptibility, is paramount to advancing our understanding of the relationship between progressive fibrosis and electrical remodeling in AF.

The focus of this study was to establish a transgenic goat (TG) model with cardiac overexpression of constitutively active TGF-β1 (αMHC-TGFcys[33]ser) and characterize the

progressive changes in cardiac structure and function in response to the transgene overexpression.

Methods

Generation of αMHC-TGFcys^{33}ser transgenic goats

Animals—Domestic goats (*Capra aegagrus hircus*) were used in this study. All animal studies were approved and monitored by the Institutional Animal Care and Use Committee (IACUC) at Utah State University (IACUC protocol # 2513) and conformed to the National Institute of Health guidelines (Guide for the Care and Use of Laboratory Animals, 8th edition). αMHC-TGFcys^{33}ser transgenic goats were generated by somatic cell nuclear transfer (SCNT) using genetically modified goat fetal fibroblasts.

Donor cells—Goat fetal fibroblasts (GFFs) were isolated from a 27-30 day old fetus as previously described.[21] Unless indicated otherwise, cell culture media and reagents were obtained from ThermoFisher Scientific. The MHC-TGF-β1cys^{33}ser fragment containing the mouse cardiac αMHC promoter and sequences encoding the human TGF-β1 cDNA was subcloned from the plasmid pUC-BM20-MHC-TGF-β1[15] into the pcDNA3.1D V5 vector as depicted in the Figure 1. The Neon™ transfection system was used to electroporate primary GFFs using 10 μg of DNA in a 100 μl tip under a 1.5 kV setting. After 2 weeks of G418 selection, the resulting G418 resistant colonies were screened by PCR to confirm transgene integration into goat genomic DNA. PCR conditions and the primer sequences are described in *the* Supplementary Materials.

Somatic cell nuclear transfer (SCNT) and embryo transfers—Transgene-positive cells, as identified by PCR, were used for SCNT to produce TGs as follows. Transgenic GFFs were grown to 90-100% confluence followed by 24 hours of serum starvation in DMEM supplemented with 0.5% FBS (HyClone) and subsequently used as nuclear donor cells. Cumulus-oocyte complexes (COCs) were recovered from abattoir-derived ovaries using a slicing technique.[22] COCs were cultured in maturation medium as described elsewhere.[23] SCNT procedure, recipient synchronization and embryo transfers were performed as previously published[21, 23] with some modification detailed in the Supplementary Materials. Female goats, 1 to 5 years of age, served as recipients for SCNT embryo implantations. The embryos were transferred into the ostium of the infundibulum via a tomcat catheter and deposited at least 3.5 cm into the oviduct. Pregnancies were diagnosed by transabdominal ultrasonography on day 35-40 of gestation.

PCR screening of cloned goats—Blood samples were collected from the resulting cloned goats to confirm the presence of the MHC-TGF-β1cys^{33}ser transgene using PCR. DNA was extracted and three sets of PCR primers were used to confirm transgene integration into the goat genome. The primer sequences and PCR conditions are described in the Supplemental Materials.

Phenotype characterization of TGF-β1 transgenic goat model

hTGF-β1 gene expression analysis—Quantitative RT-PCR was performed to measure the levels of hTGF-β1 transgene in the cardiac biopsy samples of the transgenic founder animals. The biopsies were obtained from the right ventricular (RV) septum as described in the Supplementary Materials. Additionally, qRT-PCR was used to compare the levels of hTGF-β1 expression between the atria and the ventricles of TGs. Atrial and ventricular samples were collected from both TG and wild-type (Wt) control goats. Total RNA was isolated from snap frozen tissues using the TRIzol® Plus Kit (Invitrogen). RNA concentration and purity was determined with a Nanodrop 1000 spectrophotometer (Thermo Fisher Scientific), and RNA integrity was assessed using an Agilent 2100 Bioanalyzer (Agilent Technologies). The samples were amplified in triplicates. All gene expression levels were quantified and normalized in each sample using four housekeeping genes (Beta-actin, YWHAZ, EIF4A, and GAPDH). Because the Wt control samples had no expression of the transgene, hTGF-β1 expression in the founder animals was calculated as a percentage of expression relative to the housekeeping genes. For the comparison of the transgene expression between the atria and the ventricles, relative quantification (fold change (FC)) was calculated using $2^{-\Delta\Delta Ct}$ method.[24] Primers sequences and qRT-PCR conditions are provided in the Supplemental Materials.

Surface ECG—ECG signals were collected using PowerLab hardware and associated LabChart 7 software (v7.3.7, ADInstruments) connected to restrained animals via surface electrodes (a modified Lead II ECG - back of the neck to right leg). ECGs were collected at 6, 12, 18, 24 and 36 months of age, and 10 to 50 noise free sinus beats were analyzed for each animal. QRS intervals, heart rate and P-wave durations were calculated and compared between TGs and their age, sex and weight matched Wt controls. Effect of age on these parameters was also assessed.

Echocardiography—Images were acquired from not sedated goats using a Vivid-q ultrasound system (GE HealthCare). The examination was performed with the goat in right lateral recumbency with the right front leg extended. A complete right-parasternal two-dimensional, M-mode, and color Doppler examination was performed as previously described.[25] All variables were measured three times on three different cycles to calculate an average for each variable. The list of recorded measurements is included in Table 1 *and the* Supplementary Materials. Systolic function was evaluated using percent fractional shortening calculated from M-mode images of the left ventricle and using percent ejection fraction using the Teicholz method. Diastolic function could not be consistently evaluated due to the high variability and poor repeatability of pulsed wave Doppler imaging reported in goats.[26] Additionally, left parasternal apical views could not be obtained due to gas in the reticulo-rumen [26] and other methods of diastolic function measurements, such as speckle tracking and strain imaging, have not been validated in goats.

AF induction study—AF inductions were conducted by either RAP or premature atrial stimulation using a quadripolar catheter placed in the right atrium (RA). Each method of induction was tested three times. RAP at twice the stimulation threshold strength at 50Hz for 30 seconds was used. For premature atrial stimulation, a single premature stimulus was

given after a train of eight pacing pulses. The coupling interval of the premature beat was reduced starting at 200 ms in 10 ms increments until atrial capture was lost. Atrial intracardiac electrograms were recorded by another quadripolar catheter in the RA. Sustained AF was defined as an episode of rapid irregular atrial rhythm lasting more than 2 minutes after termination of induction. An animal exhibiting sustained AF following an induction was considered AF susceptible. AF episodes lasting longer than 10 minutes were cardioverted with a 100 J external shock.

Confocal Imaging—RV biopsies were collected during AF inducibility studies using a bioptome under intra-cardiac echocardiogram and fluoroscopy guidance (see Supplementary Materials for details). The biopsies were formalin-fixed and cryo-sectioned into 100 μm thick sections and subsequently labeled with wheat germ agglutinin (WGA) conjugated to CF488 (WGA, Biotium 29022, 40 μg/ml in PBS). Three-dimensional image stacks were acquired with a Zeiss LSM 5 confocal microscope (Carl Zeiss) using a 40× oil immersion lens and an excitation wavelength of 488 nm. Stack sizes were typically 1024×1024×250 voxels with a voxel size of 0.2×0.2×0.2 μm. Preprocessing of these images involved noise reduction and deconvolution as described previously.[27] A threshold of histogram mode plus one standard deviation was applied to the preprocessed image[28] yielding the volume fraction of extracellular matrix (ECM) including fibrotic tissue.

TGF-β1 protein analysis—Concentrations of TGF-β1 were determined using a Human/Mouse TGF-β1 ELISA Ready-Set-Go kit (eBioscience, San Diego, CA) according to the manufacturer's protocol (see Online Supplementary Materials for details). The samples were tested in triplicate. Human TGF-β1 standards were run in duplicate two-fold dilutions ranging from 1,000 to 15.6 pg/ml. The plate was read at 450 and 560 nm. The TGF-β1 OD values were obtained by subtraction of the 560 nm background values from the 450 nm values. The concentration of TGF-β1 was calculated based on the TGF-β1 standard curve. Data were normalized by calculating the concentration of TGF-β1 in picograms per milligram of total protein.

Histology and morphometry—For histology, samples were collected following euthanasia that was performed using an overdose of sodium pentobarbital administered intravenously at a dose of 40 mg/kg. Formalin-fixed heart sections were processed and embedded in paraffin according to routine histologic techniques. Sections, 5-μm thick, were stained with hematoxylin and eosin (H&E) and Masson's trichrome stain according to standard methods, and examined by light microscopy.[29] For each section, 10 randomly selected sites were photographed at 400× using an Olympus DP 26 digital microscope camera with CellSens digital imaging software mounted on an Olympus BX 43 microscope (Olympus Corporation**).** The amount of fibrosis in heart sections was determined by measuring the percentage area occupied by blue staining using Photoshop CS6 (Adobe Systems). The images were manually thresholded and the same threshold setting was used for all images.

The cardiomyocyte diameter was assessed by measuring the distance across the cell at its narrowest plane across the nucleus for 100 cells from each atrium and ventricle.

Statistical analysis—All data are presented as mean±SEM.

ECG data analysis: Age-specific analyses comparing data between TGs and Wt controls were performed using a classical ANOVA model where assumptions were satisfied; a Bonferroni correction was applied across the age levels. A repeated measures model (with age and subject effects) was used specifically for P-wave duration data.

TGF β-1 gene expression: T test was used to compare ΔCt values between the TG and Wt control groups.

Echocardiography, TGF β-1 protein analysis, histology and morphometry: The nonparametric Wilcoxon Rank-Sum test was applied to the data and Bonferroni correction (across the variables/ heart chambers tested) was used to adjust for multiple comparisons.

Confocal data analysis: The measurements were averaged within each goat due to the technical nature of replication. Pairwise comparisons between age/group combinations were tested in an ANOVA model with Tukey's adjustment for multiple comparisons.

AF induction test: TGs and Wt control goats were assessed for AF susceptibility (+) or (−) response following AF induction tests. A Fisher's Exact Test was used to determine whether the response rate was the same for these two groups.

Results

Generation of TGF-β1cys^{33}ser transgenic goats

Fourteen embryo transfers were initially performed and 5 recipient goats (36%) were confirmed to be pregnant. All pregnancies had normal gestation length (147-153 days) and resulted in birth of 7 female offspring (two sets of twins and three singletons). PCR analysis revealed that 6 of the 7 goats produced by SCNT were transgenic for hTGF-β1, but only 4 (TG12, TG16, TG18 and TG20) contained both TGF-β1 and at least 1173bp of the αMHC promoter region (Figure 2. A-C). Cardiac and skeletal muscle biopsies were collected from each of the cloned goats at 12±2 months of age to measure mRNA expression of hTGF-β1. Gene expression analysis revealed that TG12, TG16, TG18 and TG20 expressed hTGF-β1 mRNA in a cardiac specific manner. The other 3 cloned goats had undetectable levels of hTGF-β1 expression. Only 4 hTGF-β1 expressing goats were used for sequential studies. None of the TGs expressed hTGF-β1 in their skeletal muscle (not shown). TG12 had the highest level of hTFG-β1 mRNA expression among the group (Figure 2.D). Different levels of hTGF-β1 gene expression are not surprising as random integration was used for production of these TGs.

To expand the number of TGs, skin biopsy samples were collected from the transgene expressing animals for fibroblast isolation and the cells were subsequently used for a second round of SCNT as depicted in Supplemental Figure 1.B. Four of 15 embryo recipients used in the re-cloning round (26.7%) became pregnant and delivered 4 transgenic females. Three of them were originated from TG12: TG12-1, TG12-2 and TG12-3 and one from TG18: TG18-1. All 4 of these animals derived by re-cloning expressed hTGF-β1 ranging from 0.14

to 1.27% of housekeeping genes (0.47± 0.53%). Thus, the total number of hTGF-β1 transgenic goats was increased to 8 animals, which were subsequently used for hTGF-β1cys^{33}ser goat model characterization.

Prolonged P-wave durations observed in TGF-β1cys^{33}ser transgenic goats

Heart rate, P-wave duration and QRS interval measurements were collected at five different time points for TGs and Wt controls. P-wave durations were significantly greater in TGs compared to Wt controls in all age groups except for the 6-month-old group (Figure 3). There was a significant age effect on P-wave duration in the TGs, but not the Wt controls between 12 and 36 months. No significant differences were found between TG and Wt groups in either QRS intervals or heart rates, regardless of the age (Supplemental Table 1).

Echocardiographic evaluation

Echocardiographic evaluation was performed on 8 TGs and 8 Wt female goats at 24±4 months of age (Table 1). After applying the Bonferroni correction, only two parameters were significantly different between the two groups: IVSs and IVSd, which suggest mild thickening of the interventricular septum.

AF induction study

Eight TGs and 6 Wt control goats were subjected to AF inducibility testing at 12±2 months of age. The TGs and Wt animals weighed 30.6±2.9 kg and 32.0±1.5 kg, respectively. While 6 of 8 (75%) TGs were susceptible to AF induction and had occurrences of sustained AF, none of the 6 Wt controls exhibited sustained AF ($P < 0.01$). Four of the 6 AF inducible TGs had AF episodes lasting at least 10 minutes that required cardioversion. In contrast, Wt goats exhibited either a single extra beat to a few seconds of AF with the longest episode lasting only 12 seconds (Figure 4). The mean AF duration of induced AF episodes was significantly greater in TGs compared to controls (687±212.0 seconds vs. 2.50±0.88 seconds, respectively; $P < 0.0001$). The AF durations in TGs were underestimated, as AF episodes lasting more than 10 minutes were typically cardioverted. In one occurrence, TG12 was not cardioverted and remained in AF for over 16 hours followed by spontaneous AF termination.

Confocal microscopy

While the increase in the ECM volume fraction in RV biopsies was not statistically significant at 12 months, the difference between Wt controls and TGs was more pronounced (+30.3%) in a subset of the same animals at 18 months of age (21.94±1.13% vs. 28.58±2.83%, respectively; $P < 0.05$) (Supplemental Figure 2). In contrast, the ECM volume fraction did not change in Wt controls between 12 and 18 months (21.18±0.35 and 21.94±1.13; $P=0.95$). The findings suggest progressive structural remodeling of cardiac tissue over time in these TGs.

Histopathology and morphometry

Samples for histology, morphometry and TGF-β1 protein analysis were collected from three TGs (TG12-1, TG12-3, TG18) at 24±4 months of age and compared to four corresponding Wt controls. One of the transgenic animals died spontaneously at 20 months of age and the

other 2 were sacrificed for sample collection. Histopathology using Masson's trichrome stain demonstrated a significant increase in diffuse collagenous stroma in the atria of TGs (Figure 5, A-B) compared to controls (11.01±2.87% and 3.08±0.77%; $P < 0.01$). A mild to severe increase in collagenous stroma was found in the endo and perimysium throughout the whole thickness of the atrial wall. No significant difference in fibrosis level was observed between LA and RA or LV and RV in the TGs. A mild multifocal increase in collagenous stroma was visually observed in the ventricles of TGs compared to controls (Figure 5, C-D); however, this difference was not significant (2.36±0.95% and 0.49±0.09%; P=0.061). After multiple comparison correction, significance threshold was 0.05/2 = 0.025. In the ventricles, the increase in endo and perimysial collagenous stroma was marginal, with the most pronounced change towards the epicardial surface and the coronary groove.

Additionally, a significant increase in the cardiomyocyte diameter was detected in the atria (20.18±1.10 μm vs. 15.72±0.42 μm; $P < 0.01$, Figure 5. E-F), but not in the ventricles (22.55±1.60 μm vs. 19.00±0.96 μm, P=0.11) of the TGs compared to controls. Even though no significant difference in fibrosis and myocyte diameter was observed in the ventricles between TG and Wt controls, there is a trend of increased levels of these parameters in the TG ventricles compared to Wt controls. Considering the limited statistical power of the study, this trend warrants further assessment.

TGF-B1 gene expression and protein analysis

Quantitative RT-PCR was conducted on atrial and ventricular samples collected from five Wt controls and 5 TGs. The analysis demonstrated that hTGF-β1cys^{33}ser expression was similar in the TGs atria and ventricles (P=0.82; FC=0.76 in ventricles compared to atria). Transgene expression was not detected in the atria and the ventricles of Wt control goats.

Total TGF-β protein content was 2.75-fold greater in the atria and about 1.84-fold greater in the ventricles of the TGs compared to the corresponding Wt controls (180.16±51.45pg/mg vs. 65.56±6.05 pg/mg; and 83.39±12.69 pg/mg vs. 45.31±4.28 pg/mg, respectively ($P <$ 0.025)). Interestingly, approximately a 2-fold greater level of total TGF-β1 was observed in the atria versus ventricles in the TGs (Supplemental Figure 3). Variability observed in the hTGF-β1 gene expression and protein level, and the amount of fibrosis among the TGs, are likely results of transgene random integration.

Discussion

This is the first study to generate a transgenic goat model with TGF-β1-induced atrial fibrosis leading to increased AF susceptibility. TGF-β1 is ubiquitously expressed at high levels in the heart during embryonic development and adult life in mammals.[30] TGF-β1 is a central mediator of atrial fibrosis in animal models[8, 9, 15] and human patients.[10, 31] It is established that the level of TGF-β1 (both mRNA and protein) and fibrosis are elevated in the heart of human patients with AF (recent review by Dzeshka[32]). Considering a key role of TGF-β1 in cardiac fibrosis and AF, we designed this goat model with overexpression of TGF-β1 to mimic elevated levels of TGF-β1 observed in human AF patients. Atrial fibrosis and increased AF inducibility in our TG model is similar to the previously reported TGF-β1 mouse model.[8, 15] However, large animal models of AF more closely resemble AF in

humans[13] and allow for sustained induction of AF[33] as compared to rodent models where AF episodes are transient lasting for only a few seconds.[8] Interestingly, the most studied to-date tachypacing models of AF typically show no significant increase in fibrosis.[6, 16] Atrial fibrosis is observed in several large animal models with experimentally induced pathologies such as dog and sheep models of congestive heart failure,[9] dog model of chronic atrial dilation due to mitral regurgitation[34] or sheep model of hypertension.[19] Comparative reviews of these animal models were previously reported.[13, 35] The uniqueness of our transgenic goat model is that progressive fibrosis is genetically induced and is the primary characteristic of the model. Therefore, the model can help with dissecting the relationship between atrial fibrosis and electrical remodeling in AF in human-size heart. This model provides opportunities for sequential data collections including intra-cardiac mapping and ablation treatments, which cannot be accomplished in the mouse model.

The association of fibrosis and AF is well established in both animal models of AF [8, 36] and human studies.[35, 37, 38] The degree of atrial fibrosis is related to the stage of AF with more fibrosis in persistent AF than paroxysmal AF.[37] Driven by the MHC promoter, both atrial and ventricular myocytes expressed similar levels of hTGF-β1 in this TG model. However, significant increase in fibrosis was only present in the atria ($P < 0.01$), which is similar to the previously developed mouse model.[15] We found an increased volume ratio of ECM in the ventricles, and quantitative increase in the level of ventricular fibrosis in TG compared to Wt controls (2.36 ± 0.95% vs. 0.49 ± 0.09%); however, this difference was not significant ($P = 0.061$). The trend of potential increase in ventricular fibrosis and how it affects cardiac function in these TGs will need to be further evaluated. The molecular mechanism of selective atrial fibrosis has been recently examined in the mouse model of TGF-β1 overexpression.[10] In the mouse model, the transcription factor AP-1 is selectively modulated by TGF-β1 in atria as evident by upregulation of AP-1 controlled genes in the atria, but not in the ventricles. Eighty genes (many of which are mediators of fibrosis) are differentially expressed in the atria and only two genes in the ventricles in the TGF-β1 mouse model.[10] Additionally, Smad2 phosphorylation was significantly increased in the transgenic atria, but not in the ventricles indicating that atrial susceptibility to TGF-β1-induced fibrosis is due to modulators of TGF-β1 receptor binding or modifiers of receptor kinase activity.[10] Further molecular characterization will be required to confirm if atrial fibrosis in the TG model has a similar molecular basis as in the mouse model. Enhanced reactivity of atrial fibroblasts compared to their ventricular counterparts could be an additional contributing factor to increased atrial fibrotic remodeling.[39] In our TG study, the increase in fibrotic content in the atrium was averaging 11%, which is in the range of fibrosis seen in patients with paroxysmal AF.[37]

This TG model had significantly greater susceptibility to AF than the Wt controls. The length of AF episodes in the Wt controls averaged 2.5 seconds, which is similar to those previously reported in goats (5 seconds),[33] dogs (7 seconds)[9] and sheep (2 seconds).[19] Both frequency and length of AF episodes were significantly greater in TGs compared to the Wt controls. The length of the AF episodes in TGs is likely to be markedly underestimated as cardioversion was typically used if AF episodes persisted longer than 10 minutes. When one of our TGs (TG12) was allowed to stay in AF following a brief 30 second RAP induction, the animal remained in a sustained AF for over 16 hours. In the classic ‘AF begets AF’ goat

study,[33] even after 24 hours of continuous rapid pacing the AF episode length only averaged 20 seconds. This suggests that fibrosis played a significant role in sustaining AF in our TG model and could be an important predictor of AF vulnerability in human patients. The lack of persistent or permanent AF indicates that although these TGs have a permissive substrate for prolonging AF episode duration, additional electrical remodeling is required for AF initiation and continuous maintenance.

The P-wave durations increased progressively between 12 and 36 months of age in TGs, while this parameter did not change in the control group. P-wave prolongation is commonly viewed as a marker of altered atrial conduction and an intermediate step that ultimately leads to AF.[40] Reports for various cardiac conditions have shown that the risk of AF is associated with prolongation of the P-wave.[40, 41] As these animals aged, the extent of structural remodeling increased as evidenced by the progressive increase in the P-wave duration.

Human and animal studies suggest that atrial remodeling increases complexity of the electrical activity in AF and leads to uncoupling of layers or muscle bundles in the atrial wall.[42, 43] This TG model with increased levels of fibrosis in the atrial wall provides a platform to study this in greater detail. The lack of significant chamber enlargement in our model supports the hypothesis that fibrosis is the primary predisposing factor for occurrence of sustained AF. The approach of targeting fibrotic regions or impacting fibrotic deposition for managing AF may lead to improved treatment outcomes, as the standard practice of performing an anatomically guided ablation isolating the pulmonary veins has not been very successful in managing persistent AF.[44] Finding new targets for ablation is a subject of intense research and different approaches have been tested such as targeting areas of complex fractionated atrial electrograms (CFAEs), creating lesions beyond the pulmonary vein isolation[45] or targeting drivers of AF such as rotors. These investigations are ongoing, but there is only a weak mechanistic basis for targeting these additional areas. Recent studies indicated that identifying stable rotors that drive AF and targeting them improves clinical outcomes.[46] It is plausible that areas of fibrosis anchor these rotors. Thus, a large animal model with fibrosis provides a critical foundation for exploration of the mechanistic basis for AF, as well as testing of novel target areas for ablation.

Conclusion

Marked atrial fibrosis, P-wave prolongation and a significant increase in AF susceptibility (following a brief electrical induction) are the primary hallmarks of this TGF-β1 transgenic goat model. In humans, the prevalence of AF increases with age due to atrial substrate remodeling developing slowly over many decades of life. This TG for the first time provides a large animal model where progressive accumulation of fibrosis creates the basis for developing AF. Serial electrophysiological studies done over time with fibrosis progression in this model can lead to further mechanistic understanding of AF. We suggest that these studies will open new clinically relevant mechanism-based targets for the prevention and treatment of AF.

Supplementary Material

Refer to Web version on PubMed Central for supplementary material.

Acknowledgements

We thank Dr. Loren J. Field for providing us with the pUC-BM20-MHC-TGF-β1 plasmid, Dr. Kerry Rood for assisting with embryo transfer procedures, and Kirsten Gash, Min Yang, Lihong Teng, Jose Reyes, Caleb Gwilliam, Sara Behunin, and David Forrester for their excellent technical assistance.

This work was supported by a grant from the Utah Science Technology and Research initiative provided to the Utah Multidisciplinary Arrhythmia Consortium [to I.A.P., R.R., C.J.D., D.J.D., R.S.M., N.M., A.L.O., and K.L.W.]; the American Heart Association [13GRNT16850082 to I.A.P.]; and the National Institute of Health [K23HL115084 to R.R.]. This research was also supported by the Utah Agricultural Experimental Station [to I.A.P.] and approved as journal paper #8786. We also acknowledge funding by the Nora Eccles Treadwell Foundation [to F.B.S. and T.S].

Abbreviations

AF	atrial fibrillation
α-MHC	alpha-myosin heavy chain promoter
ECG	electrocardiogram
ECM	extracellular matrix
RAP	rapid atrial pacing
SCNT	somatic cell nuclear transfer
TGF-β	Transforming Growth Factor-beta

References

[1]. Andrade J, Khairy P, Dobrev D, Nattel S. The clinical profile and pathophysiology of atrial fibrillation: relationships among clinical features, epidemiology, and mechanisms. Circ Res. 2014; 114:1453–1468. [PubMed: 24763464]

[2]. Weerasooriya R, Khairy P, Litalien J, Macle L, Hocini M, Sacher F, Lellouche N, Knecht S, Wright M, Nault I, Miyazaki S, Scavee C, Clementy J, Haissaguerre M, Jais P. Catheter ablation for atrial fibrillation: are results maintained at 5 years of follow-up? J Am Coll Cardiol. 2011; 57:160–166. [PubMed: 21211687]

[3]. Winkle RA, Mead RH, Engel G, Patrawala RA. Long-term results of atrial fibrillation ablation: the importance of all initial ablation failures undergoing a repeat ablation. Am Heart J. 2011; 162:193–200. [PubMed: 21742108]

[4]. Khan R, Sheppard R. Fibrosis in heart disease: understanding the role of transforming growth factor-beta in cardiomyopathy, valvular disease and arrhythmia. Immunology. 2006; 118:10–24. [PubMed: 16630019]

[5]. Tan AY, Zimetbaum P. Atrial fibrillation and atrial fibrosis. J Cardiovasc Pharmacol. 2011; 57:625–629. [PubMed: 21633248]

[6]. Li D, Fareh S, Leung TK, Nattel S. Promotion of atrial fibrillation by heart failure in dogs: atrial remodeling of a different sort. Circulation. 1999; 100:87–95. [PubMed: 10393686]

[7]. Guerra JM, Everett TH, Lee KW, Wilson E, Olgin JE. Effects of the gap junction modifier rotigaptide (ZP123) on atrial conduction and vulnerability to atrial fibrillation. Circulation. 2006; 114:110–118. [PubMed: 16818812]

[8]. Verheule S, Sato T, Everett Tt, Engle SK, Otten D, Rubart-von der Lohe M, Nakajima HO, Nakajima H, Field LJ, Olgin JE. Increased vulnerability to atrial fibrillation in transgenic mice with selective atrial fibrosis caused by overexpression of TGF-beta1. Circ Res. 2004; 94:1458–1465. [PubMed: 15117823]

[9]. Lee KW, Everett THt, Rahmutula D, Guerra JM, Wilson E, Ding C, Olgin JE. Pirfenidone prevents the development of a vulnerable substrate for atrial fibrillation in a canine model of heart failure. Circulation. 2006; 114:1703–1712. [PubMed: 17030685]

[10]. Rahmutula D, Marcus GM, Wilson EE, Ding CH, Xiao Y, Paquet AC, Barbeau R, Barczak AJ, Erle DJ, Olgin JE. Molecular basis of selective atrial fibrosis due to overexpression of transforming growth factor-beta1. Cardiovasc Res. 2013; 99:769–779. [PubMed: 23612580]

[11]. Gramley F, Lorenzen J, Koellensperger E, Kettering K, Weiss C, Munzel T. Atrial fibrosis and atrial fibrillation: the role of the TGF-beta1 signaling pathway. Int J Cardiol. 2010; 143:405–413. [PubMed: 19394095]

[12]. Polyakova V, Miyagawa S, Szalay Z, Risteli J, Kostin S. Atrial extracellular matrix remodelling in patients with atrial fibrillation. J Cell Mol Med. 2008; 12:189–208. [PubMed: 18194448]

[13]. Nishida K, Michael G, Dobrev D, Nattel S. Animal models for atrial fibrillation: clinical insights and scientific opportunities. Europace. 2010; 12:160–172. [PubMed: 19875395]

[14]. Olgin JE, Verheule S. Transgenic and knockout mouse models of atrial arrhythmias. Cardiovasc Res. 2002; 54:280–286. [PubMed: 12062333]

[15]. Nakajima H, Nakajima HO, Salcher O, Dittie AS, Dembowsky K, Jing S, Field LJ. Atrial but not ventricular fibrosis in mice expressing a mutant transforming growth factor-beta(1) transgene in the heart. Circ Res. 2000; 86:571–579. [PubMed: 10720419]

[16]. Ausma J, Litjens N, Lenders MH, Duimel H, Mast F, Wouters L, Ramaekers F, Allessie M, Borgers M. Time course of atrial fibrillation-induced cellular structural remodeling in atria of the goat. J Mol Cell Cardiol. 2001; 33:2083–2094. [PubMed: 11735256]

[17]. Verheule S, Tuyls E, Gharaviri A, Hulsmans S, van Hunnik A, Kuiper M, Serroyen J, Zeemering S, Kuijpers NH, Schotten U. Loss of continuity in the thin epicardial layer because of endomysial fibrosis increases the complexity of atrial fibrillatory conduction. Circ Arrhythm Electrophysiol. 2013; 6:202–211. [PubMed: 23390124]

[18]. Biernacka A, Frangogiannis NG. Aging and Cardiac Fibrosis. Aging and disease. 2011; 2:158–173. [PubMed: 21837283]

[19]. Kistler PM, Sanders P, Dodic M, Spence SJ, Samuel CS, Zhao C, Charles JA, Edwards GA, Kalman JM. Atrial electrical and structural abnormalities in an ovine model of chronic blood pressure elevation after prenatal corticosteroid exposure: implications for development of atrial fibrillation. Eur Heart J. 2006; 27:3045–3056. [PubMed: 17098760]

[20]. Anter E, Jessup M, Callans DJ. Atrial fibrillation and heart failure: treatment considerations for a dual epidemic. Circulation. 2009; 119:2516–2525. [PubMed: 19433768]

[21]. Keefer CL, Baldassarre H, Keyston R, Wang B, Bhatia B, Bilodeau AS, Zhou JF, Leduc M, Downey BR, Lazaris A, Karatzas CN. Generation of dwarf goat (Capra hircus) clones following nuclear transfer with transfected and nontransfected fetal fibroblasts and in vitro-matured oocytes. Biol Reprod. 2001; 64:849–856. [PubMed: 11207200]

[22]. Pawshe CH, Totey SM, Jain SK. A comparison of three methods of recovery of goat oocytes for in vitro maturation and feritilization. Theriogenology. 1994; 42:117–125. [PubMed: 16727518]

[23]. Reggio BC, James AN, Green HL, Gavin WG, Behboodi E, Echelard Y, Godke RA. Cloned transgenic offspring resulting from somatic cell nuclear transfer in the goat: oocytes derived from both follicle-stimulating hormone-stimulated and nonstimulated abattoir-derived ovaries. Biol Reprod. 2001; 65:1528–1533. [PubMed: 11673271]

[24]. Livak KJ, Schmittgen TD. Analysis of relative gene expression data using real-time quantitative PCR and the 2(T)(-Delta Delta C) method. Methods. 2001; 25:402–408. [PubMed: 11846609]

[25]. Thomas WP, Gaber CE, Jacobs GJ, Kaplan PM, Lombard CW, Moise NS, Moses BL. Recommendations for standards in transthoracic two-dimensional echocardiography in the dog and cat. Echocardiography Committee of the Specialty of Cardiology, American College of Veterinary Internal Medicine. Journal of veterinary internal medicine / American College of Veterinary Internal Medicine. 1993; 7:247–252.

[26]. Leroux AA, Farnir F, Moonen ML, Sandersen CF, Deleuze S, Amory H. Repeatability, variability and reference values of pulsed wave Doppler echocardiographic measurements in healthy Saanen goats. BMC veterinary research. 2012; 8:190. [PubMed: 23067875]

[27]. Savio-Galimberti E, Frank J, Inoue M, Goldhaber JI, Cannell MB, Bridge JHB, Sachse FB. Novel features of the rabbit transverse tubular system revealed by quantitative analysis of three-dimensional reconstructions from confocal images. Biophys J. 2008; 95:2053–2062. [PubMed: 18487298]

[28]. Schwab BC, Seemann G, Lasher RA, Torres NS, Wulfers EM, Arp M, Carruth ED, Bridge JHB, Sachse FB. Quantitative Analysis of Cardiac Tissue Including Fibroblasts Using Three-Dimensional Confocal Microscopy and Image Reconstruction: Towards a Basis for Electrophysiological Modeling. IEEE transactions on medical imaging. 2013; 32:862–872. [PubMed: 23340590]

[29]. Bancroft, J.; Gamble, M. Theory and Practice of Histological Techniques. Churchill Livingstone; 2008.

[30]. Bujak M, Frangogiannis NG. The role of TGF-beta signaling in myocardial infarction and cardiac remodeling. Cardiovasc Res. 2007; 74:184–195. [PubMed: 17109837]

[31]. Pellman J, Lyon RC, Sheikh F. Extracellular matrix remodeling in atrial fibrosis: mechanisms and implications in atrial fibrillation. Journal of molecular and cellular cardiology. 2010; 48:461–467. [PubMed: 19751740]

[32]. Dzeshka MS, Lip GY, Snezhitskiy V, Shantsila E. Cardiac Fibrosis in Patients With Atrial Fibrillation: Mechanisms and Clinical Implications. J Am Coll Cardiol. 2015; 66:943–959. [PubMed: 26293766]

[33]. Wijffels MC, Kirchhof CJ, Dorland R, Allessie MA. Atrial fibrillation begets atrial fibrillation. A study in awake chronically instrumented goats. Circulation. 1995; 92:1954–1968. [PubMed: 7671380]

[34]. Verheule S, Wilson E, Everett Tt, Shanbhag S, Golden C, Olgin J. Alterations in atrial electrophysiology and tissue structure in a canine model of chronic atrial dilatation due to mitral regurgitation. Circulation. 2003; 107:2615–2622. [PubMed: 12732604]

[35]. Burstein B, Nattel S. Atrial fibrosis: mechanisms and clinical relevance in atrial fibrillation. J Am Coll Cardiol. 2008; 51:802–809. [PubMed: 18294563]

[36]. Hanna N, Cardin S, Leung TK, Nattel S. Differences in atrial versus ventricular remodeling in dogs with ventricular tachypacing-induced congestive heart failure. Cardiovasc Res. 2004; 63:236–244. [PubMed: 15249181]

[37]. Platonov PG, Mitrofanova LB, Orshanskaya V, Ho SY. Structural abnormalities in atrial walls are associated with presence and persistency of atrial fibrillation but not with age. J Am Coll Cardiol. 2011; 58:2225–2232. [PubMed: 22078429]

[38]. Spach MS. Mounting evidence that fibrosis generates a major mechanism for atrial fibrillation. Circ Res. 2007; 101:743–745. [PubMed: 17932329]

[39]. Burstein B, Libby E, Calderone A, Nattel S. Differential behaviors of atrial versus ventricular fibroblasts: a potential role for platelet-derived growth factor in atrial-ventricular remodeling differences. Circulation. 2008; 117:1630–1641. [PubMed: 18347210]

[40]. Magnani JW, Williamson MA, Ellinor PT, Monahan KM, Benjamin EJ. P wave indices: current status and future directions in epidemiology, clinical, and research applications. Circ Arrhythm Electrophysiol. 2009; 2:72–79. [PubMed: 19808445]

[41]. Fukunami M, Yamada T, Ohmori M, Kumagai K, Umemoto K, Sakai A, Kondoh N, Minamino T, Hoki N. Detection of patients at risk for paroxysmal atrial fibrillation during sinus rhythm by P wave-triggered signal-averaged electrocardiogram. Circulation. 1991; 83:162–169. [PubMed: 1984879]

[42]. Allessie MA, de Groot NM, Houben RP, Schotten U, Boersma E, Smeets JL, Crijns HJ. Electropathological substrate of long-standing persistent atrial fibrillation in patients with structural heart disease: longitudinal dissociation. Circ Arrhythm Electrophysiol. 2010; 3:606–615. [PubMed: 20719881]

[43]. Eckstein J, Zeemering S, Linz D, Maesen B, Verheule S, van Hunnik A, Crijns H, Allessie MA, Schotten U. Transmural Conduction Is the Predominant Mechanism of Breakthrough During Atrial Fibrillation Evidence From Simultaneous Endo-Epicardial High-Density Activation Mapping. Circ-Arrhythmia Elec. 2013; 6:334–341.

[44]. January CT, Wann LS, Alpert JS, Calkins H, Cigarroa JE, Cleveland JC Jr. Conti JB, Ellinor PT, Ezekowitz MD, Field ME, Murray KT, Sacco RL, Stevenson WG, Tchou PJ, Tracy CM, Yancy CW, American College of Cardiology/American Heart Association Task Force on Practice G. 2014 AHA/ACC/HRS guideline for the management of patients with atrial fibrillation: a report of the American College of Cardiology/American Heart Association Task Force on Practice Guidelines and the Heart Rhythm Society. J Am Coll Cardiol. 2014; 64:e1–76. [PubMed: 24685669]

[45]. Wu SH, Jiang WF, Gu J, Zhao L, Wang YL, Liu YG, Zhou L, Gu JN, Xu K, Liu X. Benefits and risks of additional ablation of complex fractionated atrial electrograms for patients with atrial fibrillation: a systematic review and meta-analysis. Int J Cardiol. 2013; 169:35–43. [PubMed: 24083885]

[46]. Narayan SM, Krummen DE, Shivkumar K, Clopton P, Rappel WJ, Miller JM. Treatment of atrial fibrillation by the ablation of localized sources: CONFIRM (Conventional Ablation for Atrial Fibrillation With or Without Focal Impulse and Rotor Modulation) trial. J Am Coll Cardiol. 2012; 60:628–636. [PubMed: 22818076]

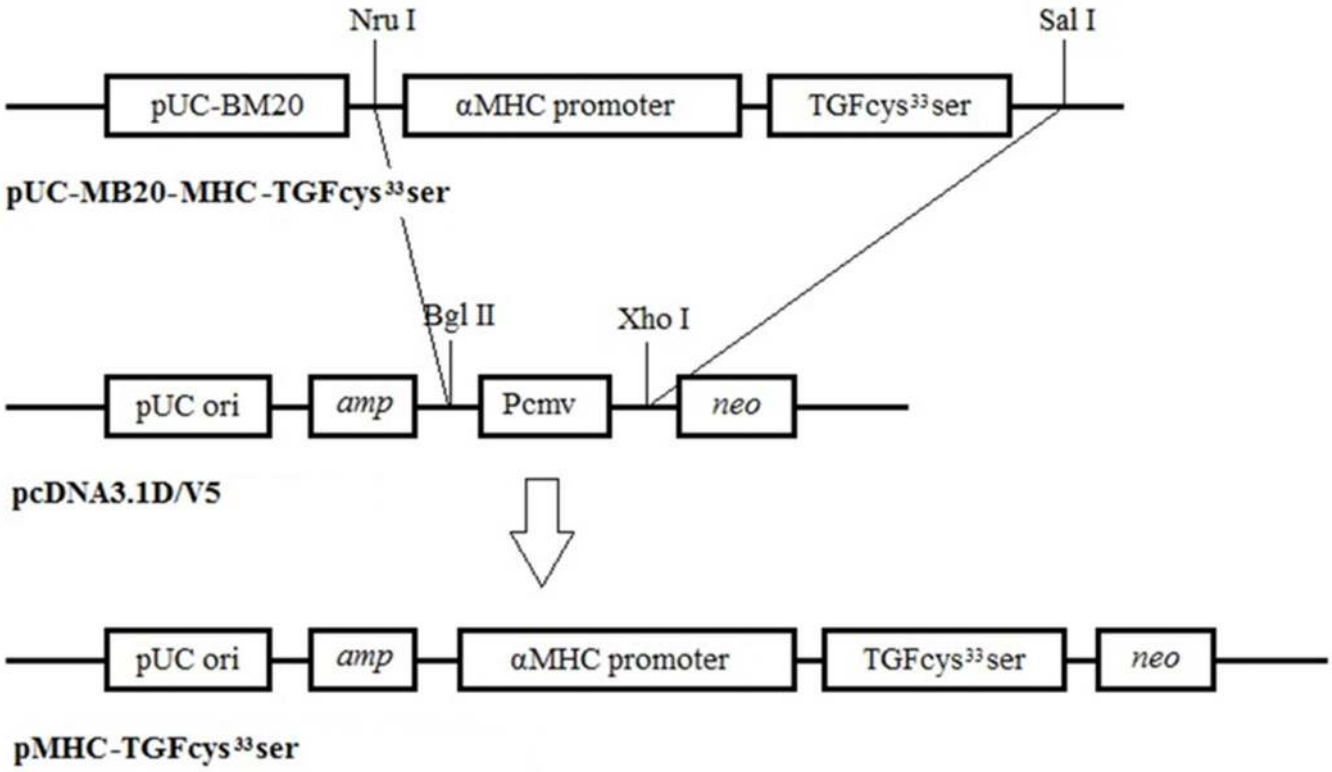

Figure 1.

pMHC-TGF-β1cys^{33}ser knock-in vector construction. The pcDNA3.1D V5 vector was linearized by digestion with Bgl II, treated with Klenow to blunt the ends, followed by cutting with Xho I; these treatments resulted in the linearized pcDNA3.1D V5 vector bearing a blunt end at the Bgl II cut site and a sticky end generated by Xho I digestion. The MHC-TGF-β1cys^{33}ser cassette was liberated from vector pUC-BM20-MHC-TGF-β1 by double digestions with Nru I and Sal I. As Nru digestion generates blunt ends and Sal I digestion generates a compatible sticky end to the sticky end generated by Xho I, the MHC-TGF-β1cys^{33}ser cassette was directly subcloned into the pcDNA3.1DV5 vector prepared above to obtain the pMHC-TGF-β1cys^{33}ser knock-in vector.

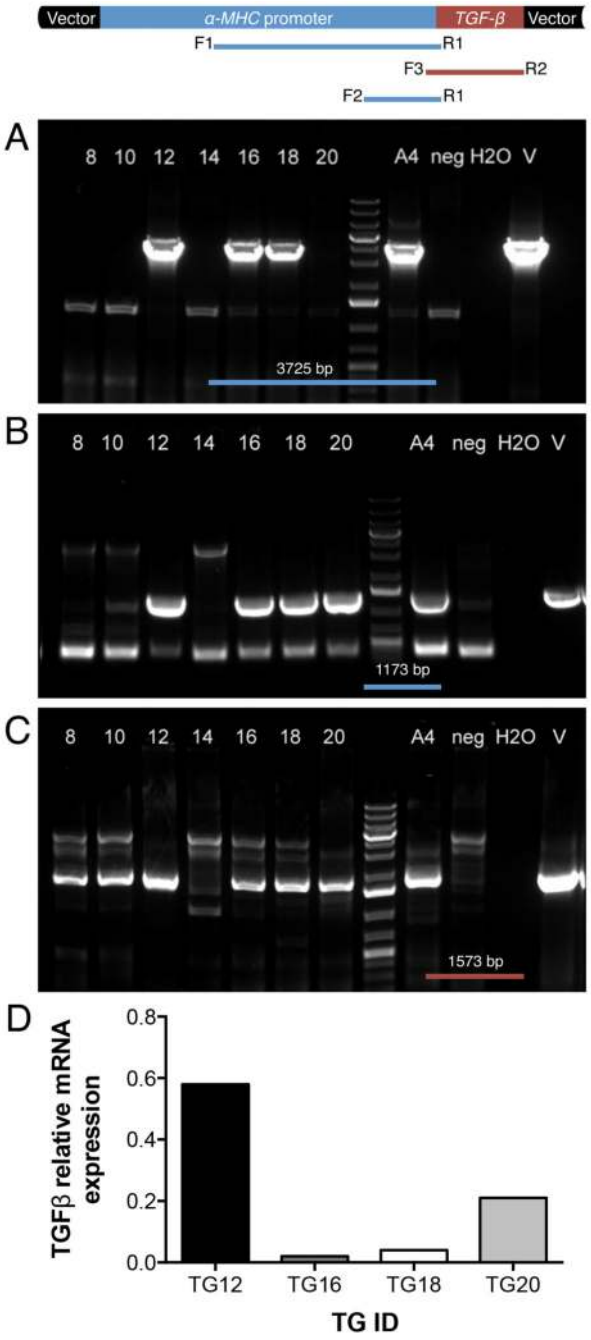

Figure 2.

A-C. PCR analysis of cloned goats. The vector cartoon is depicted above the panels. **(A)** PCR results for a 3725 bp α-MHC fragment using primers F1 and R1, **(B)** PCR results for a 1173 bp α-MHC fragment using primers F2 and R1, and **(C)** PCR results for a 1573 bp hTGF-β1 fragment using primers F3 and R2. Lanes 8, 10, 12, 14, 16, 18 and 20 = cloned goats; A4 = positive control (cells); H_2O = water only (non-template control); neg = wild-type goat genomic DNA; V = vector. **D.** *hTGFB* mRNA levels in RV biopsies of four

transgenic goats (TGs) shown as the percentage of expression relative to housekeeping genes: Beta-actin, YWHAZ, EIF4A, and GAPDH.

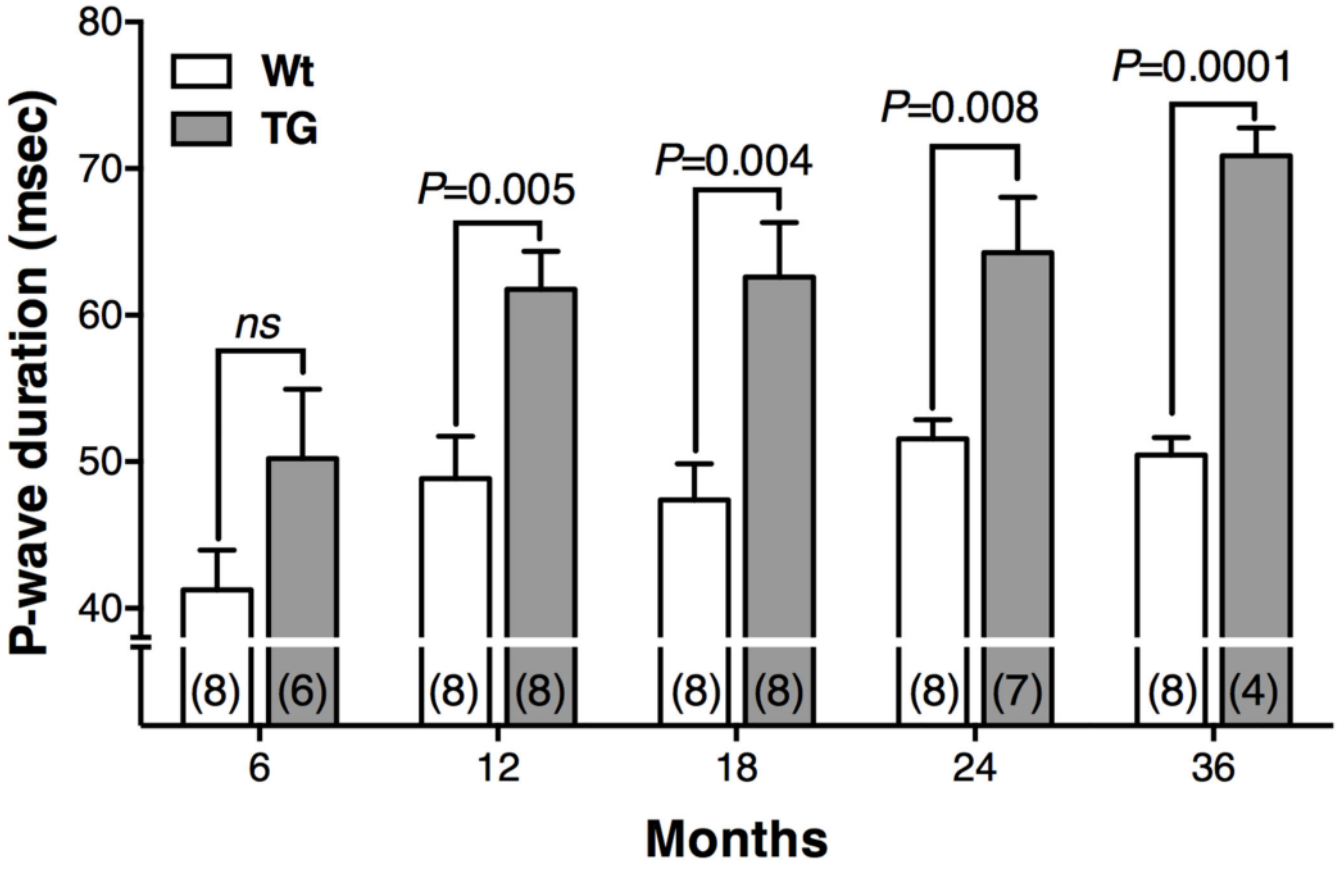

Figure 3.

P-wave duration in wild-type (Wt) and TGF-β1cys^{33}ser transgenic goats (TGs) at five different ages. Number of animals in each group is indicated in parentheses. Additional sample size information is provided in Supplemental Table 1.

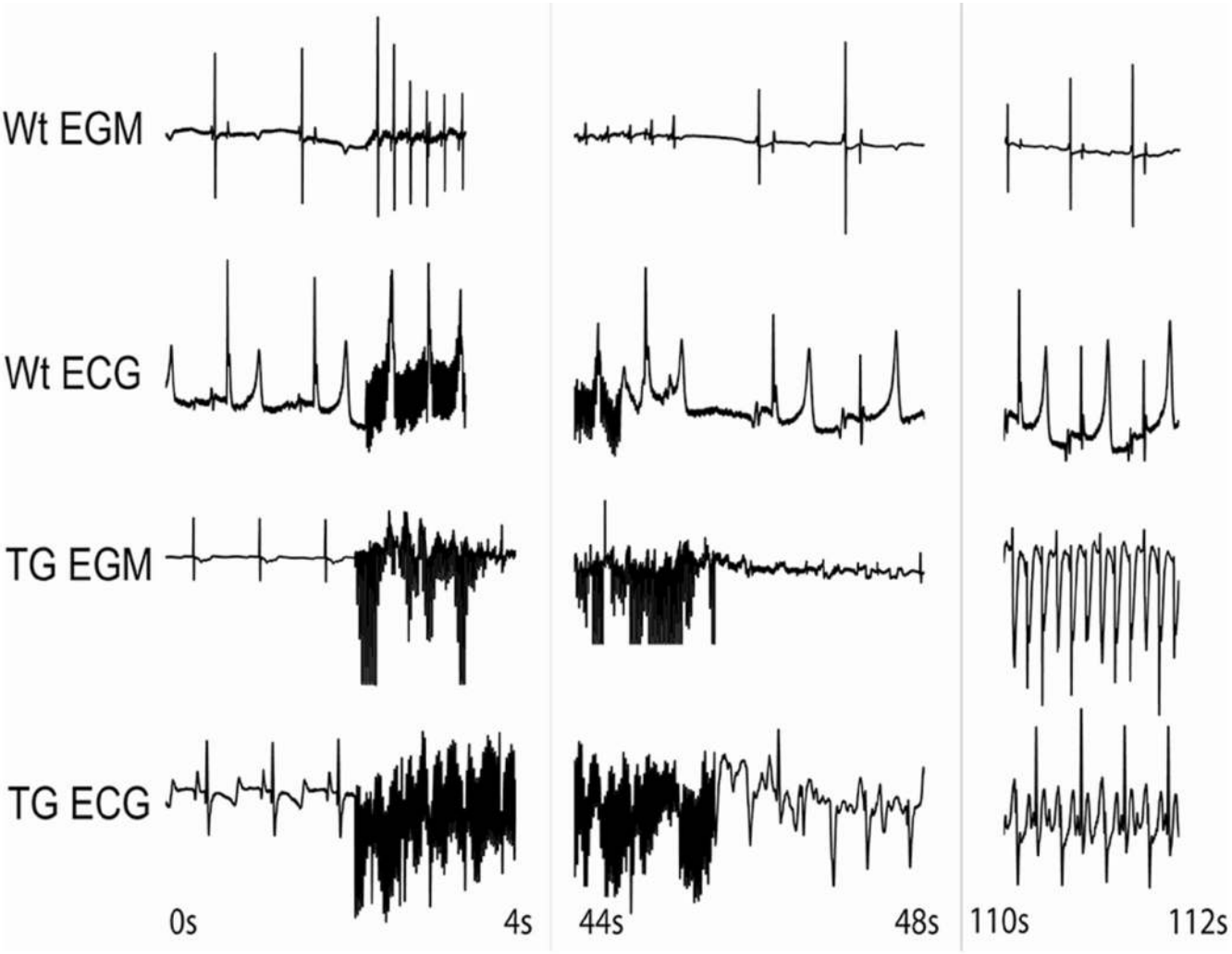

Figure 4.

Example of AF induction test following rapid atrial pacing (RAP) in a Wt and a TGF-β1cys^{33}ser TG. Shown are the bipolar atrial electrograms (EGM) and the surface electrocardiograms (ECG). The first few seconds of recording is sinus rhythm followed by RAP, which resulted in a few premature atrial contractions in the Wt control, but no sustained AF was induced. In the TG there was sustained AF lasting more than 10 minutes (not shown) requiring cardioversion. TG = transgenic goat; Wt = wild-type.

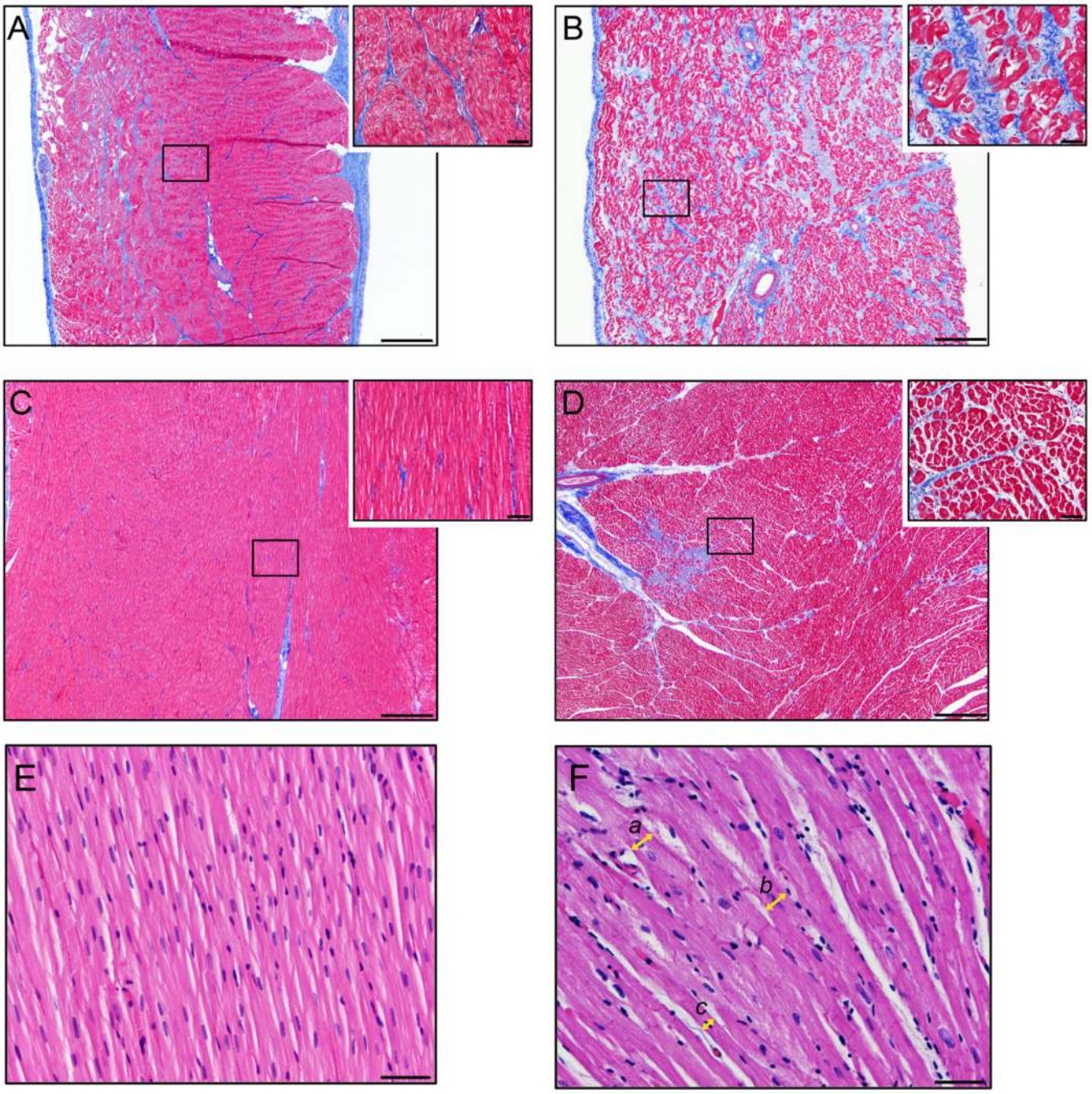

Figure 5.

Examples of histopathology of wild-type (Wt) and TFG-β1cys^{33}ser transgenic goat (TG) hearts. **A-D.** Masson trichrome stain. (**A)** Section of the left atrium (LA) of Wt heart. Note the small amount of collagenous stroma (blue staining) present in the endo and perimysium surrounding the myocytes (red staining). (**B**) Section of the LA of a TG. Note the diffusely increased amount of collagenous stroma present in the endo and perimysium compared to the control goat in A. (**C**) Section of the left ventricle (LV) of the same Wt heart as in A. (**D)** Section of the LV from the same TG heart as in B. Note the focal area with increased

amount of collagenous stroma present in the endo and perimysium compared to the control goat in C. 40× Scale bar =500 μm. Inserts: 400× Scale bar =50 μm. **E-F.** Hematoxylin and eosin stain. Histopathology of the left atrium of a Wt control goat **(E)** and TFG-β1cys^{33}ser transgenic goat **(F).** TG histopathology in **F** demonstrating myofiber hypertrophy and how the measurements of the myofiber diameter were made. Hypertrophied myofibers (***a*** *= 25.01 μm)* and *(**b** = 24.10 μm)* are present in the center and right side of the image, while myofiber with a smaller diameter (***c*** *= 13.81 μm*) similar to control animals are present in the left lower corner of the image. Myofiber diameters were measured at the narrowest plane across the nucleus. 400× Scale bar =50 μm.

Table. 1

Cardiac measurements in wild-type controls and MHC-TGFcys33ser transgenic goats

	Wt controls, n=8	MHC-TGFcys33ser TGs, n=8	*P* *
Weight, kg	39.72±3.12	39.38±4.33	0.8747
Ao Diam, cm	2.35±0.06	2.58±0.07	0.0232
LA Diam, cm	2.78±0.10	3.03±0.17	0.2879
LA/Ao	1.19±0.03	1.18±0.06	0.4302
LA Max, cm	3.93±0.09	4.43±0.23	0.0346
RA Max, cm	2.59±0.09	2.68±0.17	0.7099
Ao Max, cm	1.98±0.05	1.95±0.03	0.7025
IVSd, cm	0.75±0.03	1.09±0.07	**0.0010**
LVIDd, cm	3.73±0.13	3.81±0.16	0.6343
LVPWd, cm	0.94±0.04	1.15±0.12	0.0476
IVSs, cm	1.09±0.03	1.56±0.12	**0.0010**
LVIDs, cm	2.13±0.13	1.94±0.12	0.3898
LVPWs, cm	1.56±0.03	1.95±0.13	0.0134
EF, %	74.5±1.94	81.25±2.29	0.0455
FS, %	42.88±1.73	49.75±2.64	0.0515
RVIDd, cm	1.27±0.07	1.31±0.15	0.9580
RVIDs, cm	1.04±0.09	0.91±0.12	0.4278
RVOT Vmax, m/s	0.92±0.07	0.92±0.10	0.7525
RVOT MaxPG, mmHg	3.51±0.51	3.67±0.83	0.7527

*After applying the Bonferroni correction to adjust for multiple comparisons, significance threshold was 0.05/19 = 0.0026. Therefore, only two parameters (IVSd and IVSs) were significantly in transgenic goats compared to controls. Ao Diam = aortic diameter; Ao Max = maximal aortic diameter; EF = ejection fraction; FS = fractional shortening; IVSd = width of the interventricular septum in diastole; IVSs = width of interventricular septum in systole; LA/Ao = left atrium to aortic ratio; LA Diam = left atrial diameter; LA Max = maximal left atrial diameter; LVIDd = left ventricular internal dimensions in diastole; LVIDs = left ventricular internal dimensions in systole; LVPWd = width of left ventricular posterior wall in diastole; LVPWs = width of left ventricular posterior wall is systole; RA Max = maximal right atrial diameter; RVIDd = right ventricular internal dimension in diastole; RVIDs = right ventricular internal dimension in systole; RVOT MaxPG = maximal pressure gradient between the right ventricle and pulmonary artery (calculated using the modified Bernoulli equation, $\Delta p = 4\ (\text{velocity})^2$; RVOT Vmax = maximal velocity of blood flowing out of the right ventricular outflow tract during systole; Wt = wild-type control goats.